Physicochem. Probl. Miner. Process., 58(4), 2022, 149937

http://www.journalssystem.com/ppmp

Physicochemical Problems of Mineral Processing

ISSN 1643-1049

Effect of the oxygen-containing functional group on the adsorption of hydrocarbon oily collectors on coal surfaces

He Wan [1,2], Xianglin Hu [1], Saija Luukkanen [2], Juanping Qu [1], Chonghui Zhang [1], Jiwei Xue[1], Hui Li [3], Wei Yang [1], Shenghong Yang [2], Xianzhong Bu [1]

[1] School of Resources Engineering, Xi'an University of Architecture and Technology, Xi'an 710055, China

[2] Oulu Mining School, University of Oulu, Oulu, FI-90014, Finland

[3] College of Resource and Civil Engineering, Northeastern University, Shenyang, 110819, China

Corresponding author: wanhe@xauat.edu.cn (He Wan); buxianzhong@xauat.edu.cn (Xianzhong Bu)

Abstract: The oxygen-containing functional groups (OCFG) on the coal surface affect the adsorption effect of hydrocarbon oily collectors (HOC). An investigation of the interaction between the HOC and OCFG in the absence and presence of water is conducive to understanding the effect of OCFG type on the adsorption of HOC on the coal surface. In this paper, FTIR analysis was used to analyze the OCFG type of coal surface. The adsorption behavior of HOC on different OCFG surfaces was investigated using molecular dynamics simulation. The results indicated the presence of OCFG such as -OH, -COOH, -C=O, and -$COCH_3$ on the coal surface. In conditions without water, the effect of OCFG on HOC adsorption capability follows the order -COOH > -C=O > -OH > -$COCH_3$. In an aqueous solution, the effect of OCFG on HOC adsorption capability follows the order -C=O>-$COCH_3$>-OH>-COOH. Moreover, the hydrophilicity of OCFG is the key factor that affects the adsorption effect of HOC. In other words, the adsorption effect of HOC on the coal surface in an aqueous solution does not depend on the strength of the interaction between the OCFG and HOC in the absence of water, but on the hydrophilicity of the OCFG. The -COOH and -OH on the coal surface are not conducive to the adsorption of HOC onto the coal surface. Masking the -COOH and -OH of the coal surface is beneficial in improving the coal flotation performance with HOC as a collector.

Keywords: oxygen-containing functional groups, hydrocarbon oily collectors, molecular dynamics simulation, coal surfaces, adsorption

1. Introduction

Flotation is a method for the efficient and clean use of coal resources (Li et al., 2020a; Li et al., 2020b;). It is a technique based on the difference in surface properties between coal and minerals and being separated in a gas-liquid-solid three-phase fluid. Coal surface hydrophobicity is an important surface property that determines the flotation effect of coal slimes. In other words, the higher the hydrophobicity of the coal surface, the better the flotation effect (Xia et al., 2021; Li et al., 2020c).

The coal types are numerous. The hydrophobicity of the surface of different types of coal varies considerably. This mainly depends on the type and content of oxygen-containing functional groups (OCFG) on the surface of the coal (Wang et al., 2018). Some studies found that lignite coals contain many OCFG such as hydroxyl, carbonyl, and carboxyl on their surfaces (Zhang et al., 2018; Xia et al., 2016). Long-flame coals contain many hydroxyl and carbonyl groups on their surfaces (Qu et al., 2015). This is the main reason for the poor hydrophobicity of low-rank coals. Coking coal is bituminous with fewer OCFG on its surface and better natural hydrophobicity (Zhang and Xia, 2015). The anthracite has much lower OCFG on its surface. It also has excellent natural hydrophobicity. However, oxidation increases the OCFG content on anthracites surfaces such as hydroxyl and carboxyl, causing a decrease in its hydrophobicity (Xia et al., 2018). This is consistent with the result of Tan et al. that the higher the oxygen content in coal, the less hydrophobic surface is (Tan et al., 2020).

DOI: 10.37190/ppmp/149937

Hydrocarbon oils (e.g., kerosene or diesel) are the most common collectors for fine coal flotation (Xia et al., 2018; Harris et al., 1995). Some studies found that the adsorption rate of hydrocarbon oils on the coal surface is affected by the surface properties of the coal (Zhang et al., 2020a). Zhang et al. found that when the surface hydrophobicity of the coal is high, a good flotation performance can be achieved with a small amount of diesel (Zhang et al., 2015). Xu et al. found that the oxygen content on the surface of long-flame coal was higher than the carbon content, and the combustible recovery was only 30.14% when diesel was used at 6 kg/t (Xu et al., 2018); increasing the amount of diesel used in the flotation process helps to improve the flotation of high oxygen content coals. Xia et al. found that dodecane only interacts with nonpolar groups on the surface of low-rank coals through hydrophobic interactions and hardly interacts with polar groups on their surfaces through molecular dynamics simulations (Xia et al., 2021; Liu et al., 2019; Xia et al., 2020a; Xia et al., 2019a; Zhang et al., 2020b; Zhang et al., 2021). These indicate that OCFG on coal surfaces can limit the adsorption of hydrocarbon oils, affecting the flotation efficiency of low-rank coals (LRC) and oxidized coal (Xia et al., 2019a; Zhang et al., 2020c; Zhang et al., 2021a; Abarca et al., 2018; Carla et al., 2018; Zhou et al., 2018; Jia et al., 2000; Dey et al., 2013). In addition, Zhang et al. (2021b) further found in an aqueous solution, the oil droplet cannot spread on the –OH and –COOH surfaces, and are still clustered together in a spherical form; for –C=O and -$COCH_3$ surfaces, oil droplet spread on these surfaces, thereby forming an oil film. However, in the absence and presence of water, the effect and difference of OCFG on the adsorption of hydrocarbon oily collectors (HOC) on coal surfaces have not been reported.

Therefore, an investigation of the interaction between the HOC and OCFG in the absence and presence of water is conducive to understanding the effect of OCFG type on the adsorption of HOC on the coal surface. In this paper, Fourier-transform infrared spectroscopy (FTIR) was used to analyze the OCFG type of coal surface. The adsorption behavior of HOC on different OCFG surfaces in the absence and presence of water was investigated using molecular dynamics simulation (MDS), which included adsorption configuration, relative concentration profiles, radial distribution function, interaction energy, and mean square displacement (MSD). Coal has a complex organic structure. The coal surface contains a variety of functional groups. (Liu et al., 2019; Zhang et al., 2020a; Zhang et al., 2020c; Lyu et al., 2018; Li et al., 2020c). To reduce the interference of other functional groups on the coal surface, a single OCFG was grafted on the graphite surface for constructing the surface models. This had been confirmed to be feasible in the study of the mechanism of interaction between the flotation agent and the OCFG of the coal surface. (Xia et al., 2020a; Zhang et al., 2020a; Zhang et al., 2021a). Dodecane was used to replace the HOC in the MDS because HOC is a mixture. The results provided a new perspective for understanding the effect of OCFG type on the adsorption of HOC on the coal surface at the molecular level, which is beneficial to help analyze the reasons for the high dosage of diesel and the poor flotation performance of coal with high OCFG. It also provides theoretical support for optimizing and designing new collectors for improved flotation performance of coal with high OCFG.

2. Materials and methods

2.1. Coal sample and reagents

The LRC and CC samples from Inner Mongolia, China, were used in this study. They were the -0.5 mm coal flotation feed in Shendong (low-rank coal) and Bailing (coking coal) coal processing plants, respectively. The proximate analysis of the coal samples is given in Table 1.

Table 1. The results of proximate analysis of the coal samples (%)

Name	M_{ad}	A_{ad}	V_{ad}	FC_{ad}
LRC	2.21	24.98	25.38	47.43
CC	0.91	20.00	25.87	53.22

ad: Air-dry basis; M: Moisture; A: Ash; V: Volatile Matter; FC: Fixed Carbon.

2.2. FTIR analysis

FTIR analysis was carried out by using a Fourier transform infrared spectroscopy (Nicolet iS5, Thermo Scientific, USA). The coal samples of LRC and CC were mixed with KBr (Potassium Bromide),

respectively, then pressed to small pelletized discs for FTIR analyses conducted in the range of 400-4000 cm^{-1}.

2.3. Simulation details

In this paper, the structure of dodecane is shown in Fig. 1(a). Graphite surface structure was established based on the method of the previous studies (Xia et al., 2020a; Zhang et al., 2020a). The OCFG was grafted onto the graphite surface to simulate a coal surface with a single OCFG. The detailed construction process is shown in Fig. 1(b). Firstly, the graphite was cleaved along its (001) surface. Then, a single type of OCFG was grafted onto the graphite surface along the Z-axis at the location shown in the figure. Finally, a 10× 10 supercell (24.60 × 24.60Å^2) was constructed. In addition, to prevent the interaction between the grafting molecules, the supercell of 2×2 has a grafting site. The zoomed-in view of the graft structure of carboxyl (–COOH), hydroxyl (–OH), carbonyl (–C=O), and methyl ether (-$COCH_3$) is shown in Fig. 1(c). Correspondingly, a cell containing 5 dodecanes/ 1000 water molecules was constructed with the same dimensions as grafted graphite. A vacuum layer of 80Å was established to eliminate periodicity effects. The final model in the absence of water/ dodecane is shown in Fig. 1(d)/(e). Based on the model in the absence of water, 1000 H_2O was introduced for simulating the adsorption process of dodecane in a water environment, as shown in Fig. 1(f), and other parameters were the same. In the simulation, all graphite atoms were constrained, and the grafted OCFG, water molecules, and dodecane molecules were free to move (Zhang et al., 2021b). Before MDS, 5000 geometric optimization steps were performed to eliminate unreasonable contact between atoms.

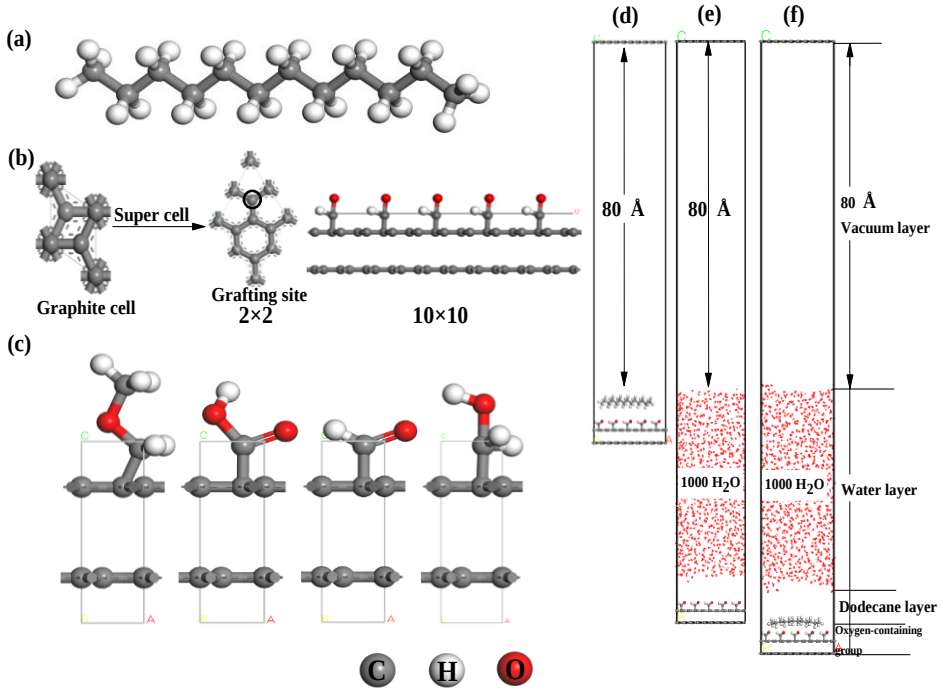

Fig. 1. Molecular structure and models: (a) Graphite grafting -$COCH_3$; graphite grafting –COOH; graphite grafting –C=O; graphite grafting –OH; (b) Dodecane; (c) OCFG model and Simulation boxes for MDS in the absence of water (d), in the absence of dodecane (e) and in the presence of water and dodecane (f).

MDS was performed using the Nosé thermostat and NVT ensemble with a one fs time step. This had been confirmed to be satisfactory for simulation requirements (Xia et al., 2020a; Zhang et al., 2020a; Zhang et al., 2021b). For the entire interaction, 2000 ps simulations were conducted. The last 100 frames are used for analysis. The Ewald/ atom-based method was used for electrostatic/ Van der Waals interactions with a 0.001 kcal/mol precision/ a cut-off of 12.5 Å. Molecular dynamics simulations were carried out using the Forcite modules of Materials studio 8.0 software. COMPASS II force-field was employed in all simulations.

3. Results

3.1. FTIR analysis

The FTIR analysis results of LRC/CC are shown in Fig. 2. As shown in Fig. 2, several absorption band for LRC/CC samples include: -OH stretching frequency around 3693cm^{-1}, 3618cm^{-1}, and 3414 cm^{-1} (He et al., 2018; Li et al., 2020c; Aljerf and Nadra, 2019; Fan et al., 2020); -CH stretching frequency at 3041 cm^{-1}, 2922 cm^{-1}, 2855 cm^{-1} (Li et al., 2020c; Li et al., 2019; Zhu et al., 2019); -COO- stretching frequency at 1735 cm^{-1}, 914 cm^{-1} (He et al., 2018; Zhu et al., 2020); -C=C- stretching frequency at 1607.69 cm^{-1} (He et al., 2018; Li et al., 2020c); -CH_3 stretching frequency at 1443 cm^{-1}, 1381 cm^{-1} (Li et al., 2020c; Zhu et al., 2020; Cai et al., 2018); -COC- stretching frequency at 1271.74 cm^{-1}, 1096.15 cm^{-1}, 1035.28 cm^{-1}, 879cm^{-1} (Li et al., 2020; He et al., 2018; Fan et al., 2020; Zhu et al., 2020; Yang et al., 2021); -C-C=O stretching frequency at 694.45 cm^{-1}, 538.01cm^{-1}, 470.47cm^{-1} (Li et al., 2020b; Fan et al., 2020; Yang et al., 2021; Marcelo et al., 2006; Xie et al., 2017; Akyıldırım et al., 2017). These indicate the presence of functional groups such as -OH, -CH, -COO-, -CH_3, -COC-, -C=O on the surface of LRC and CC. The OCFG on the coal surface are mainly carboxyl (-COOH), hydroxyl (-OH), carbonyl (-C=O), ether(-COC-).

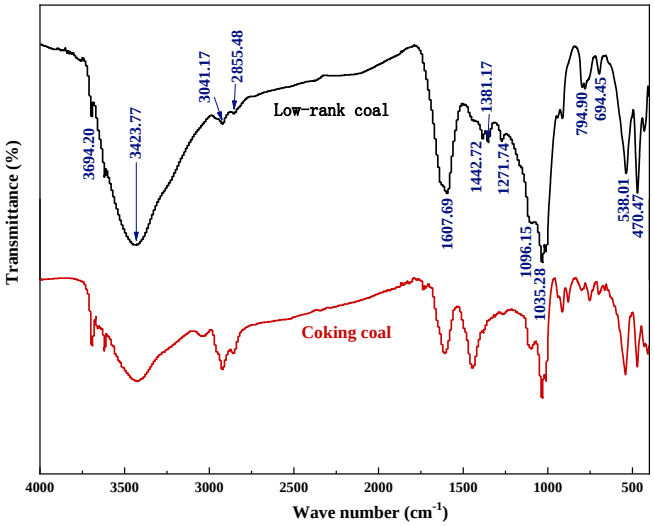

Fig. 2. FTIR analysis results

3.2. Interactions between OCFG and dodecane molecules in the absence of water

3.2.1. Adsorption configuration

Fig. 3 shows the adsorption initial and equilibrium states of dodecane on the different oxygen-containing functional groups (DOCFG) of coal surface in the absence of water. It can be observed from Fig. 3 that the dodecane molecule can be adsorbed on the OCFG in a tilted or flat manner and form an oil film. However, there is a difference in the number of layers of dodecane adsorbed on the DOCFG. Dodecane is adsorbed as a monolayer on the -COOH and -C=O surface and as multiple adsorptions on the -OH and -$COCH_3$ surface. This indicates that the absorption effect of dodecane on the -COOH and -C=O surface is better than those of the -OH and -$COCH_3$ in the absence of water.

3.2.2. Relative concentration profiles and radial distribution function

To further analyze the adsorption configuration, the relative concentration distribution and radial distribution function of dodecane molecules along the Z-axis (vertically to the surface of the OCFG model) were calculated. The results are shown in Fig. 4 and Fig. 5.

Fig. 4 shows that there were differences in the concentration of dodecane on the OCFG surface, but the differences were not significant. The relative concentration of dodecane on the DOCFG surface from low to high is -$COCH_3$<-OH<-C=O<-COOH. In other words, dodecane has the highest adsorption on -COOH and lowest adsorption on -C-O-CH_3. This result is consistent with the observed adsorption configuration result (Fig. 3).

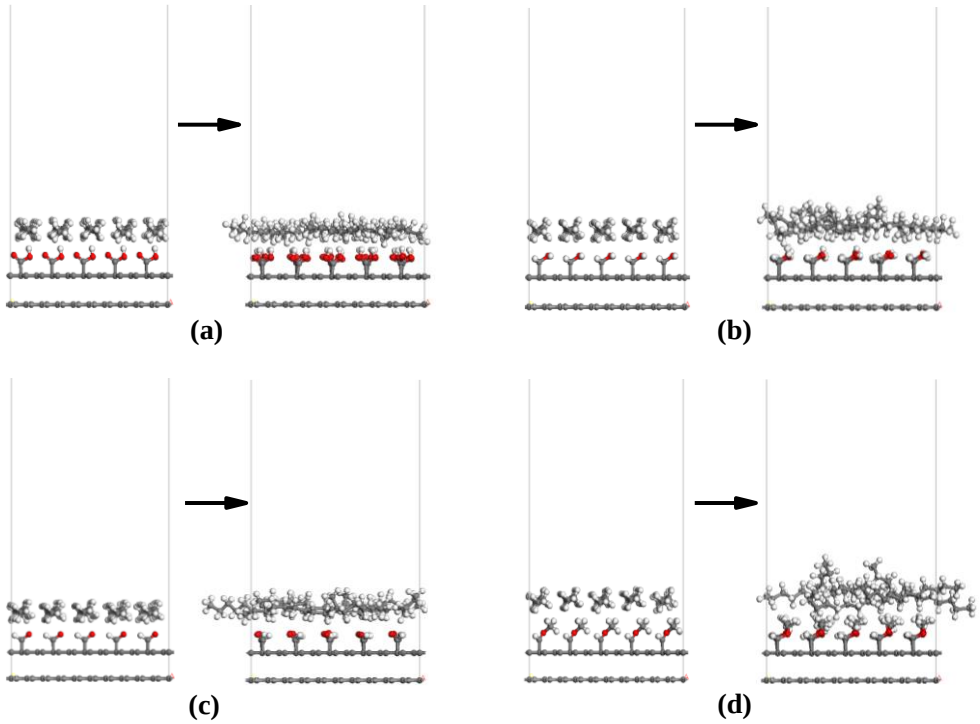

Fig. 3. The adsorption initial and equilibrium states of dodecane on the DOCFG without water (a) -COOH; (b) -OH; (c) -C=O; (d) -$COCH_3$

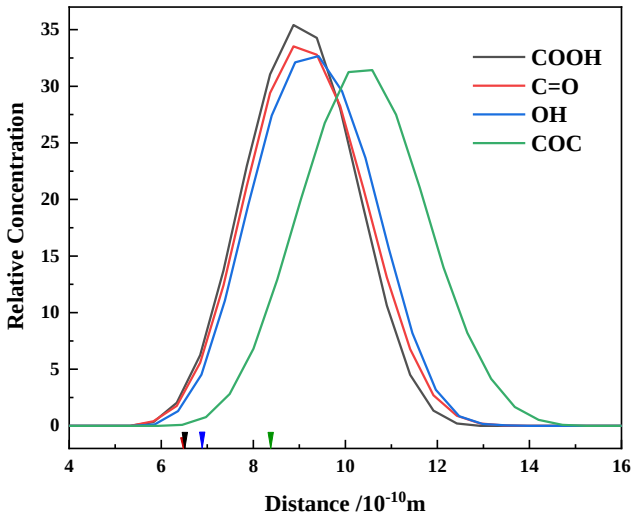

Fig. 4. The relative concentration of dodecane molecules on DOCFG

The radial distribution function (Fig. 5.) describes how the dodecane density varies as a function of distance from a dodecane molecule. Higher peaks indicate more distance between dodecanes. This also indicates the strength of the interaction between the OCFG and the dodecane in the Z-axis direction. The higher the peak is, the weaker the interaction of the OCFG with the dodecane is. As shown in Fig. 5, the positions of the radial distribution function peaks between the dodecane are the same. The difference lies in the heights of those peaks. The peak height in -$COCH_3$/-OH/-C=O /-COOH is 469.21/384.67/379.36/355.84. Therefore, the distance between the dodecane molecule order -$COCH_3$> -OH>-C=O >-COOH. This means that on the -COOH surface, the probability of finding a dodecane molecule around the dodecane molecule is the most at the same distance. The strength of the interaction between the dodecane molecule and the -COOH surface is also probably the strongest. The RDF results agree well with the results of relative concentration (Fig. 4).

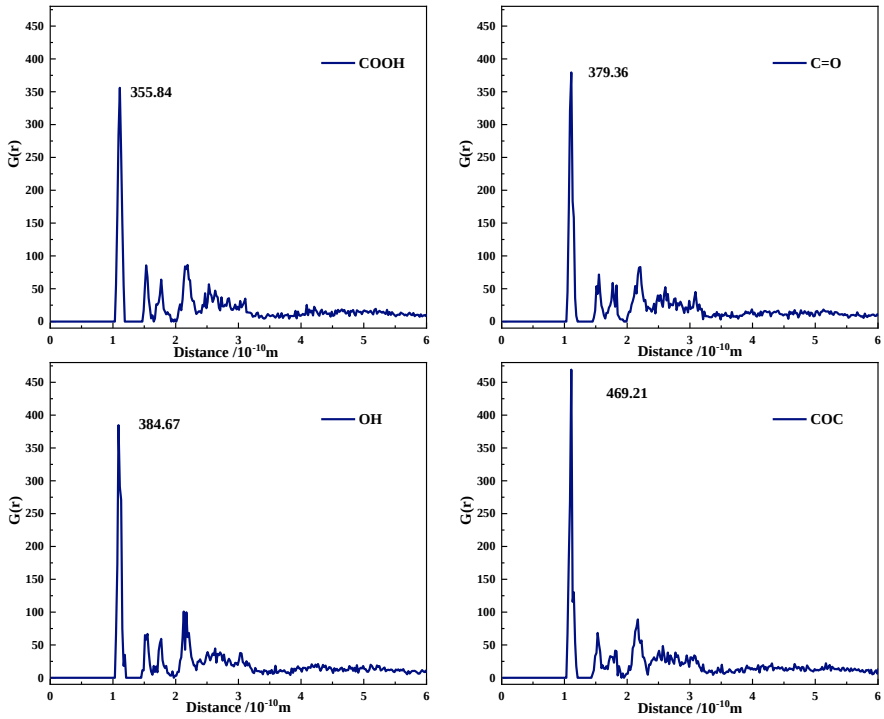

Fig. 5. Radial distribution of dodecane molecules on DOCFG

3.2.3. Interaction energy

The interaction energy (E_{int}) is used to describe the interaction intensity between dodecane molecule and OCFG surfaces. E_{int} can be computed using Eq. (1). The van der Waals energy component (E_{vdw}) and electrostatic interaction (E_{elec}) are also listed in Table 2.

$$E_{int} = E_{complex} - (E_{surface} + E_{\text{dodecane}}) \quad (1)$$

where E_{int} is the interaction energy; $E_{complex}$, $E_{surface}$, and E_{dodecane} are the energy of the complex model, coal, and dodecane, respectively.

Table 2. Interaction energies between dodecane and OCFG (KJ/mol)

OCFG	E_{int}	E_{vdw}	E_{elec}
-COOH	-83.49	-79.84	-3.65
-OH	-68.00	-67.42	-0.58
-$COCH_3$	-62.74	-62.00	-0.14
-C=O	-75.34	-74.63	-0.70

It can be seen from Table 2 that the interaction energies of dodecane with -$COCH_3$/-OH/-C=O /-COOH are -62.74 kcal.mol^{-1} /-68.00 kcal.mol^{-1} /-75.34 kcal.mol^{-1} /-83.49 kcal.mol^{-1}. Therefore, the interaction between dodecane and OCFG from low to high is -$COCH_3$<-OH<-C=O<-COOH. This result is consistent with the radial distribution function (Fig. 5.). Meanwhile, the van der Waals force does work that is very close to the interaction energy. The electrostatic force does work those only account for a tiny part. This result suggests that E_{vdW} is dominant in the adsorption of dodecane on the coal surface. The main reason accounting for this phenomenon is that the dodecane molecules cannot ionize, and then no source of electrostatic interaction (Zhang et al., 2021b).

3.2.4. The diffusion coefficients of dodecane on OCFG

The differences in the surface properties of OCFG will affect the dynamic behavior of dodecane (Li et al., 2019). MSD curves were used to analyze the kinetic properties of dodecane on OCFG. In the MSD

curves, the mobility of dodecane is affected by the type of OCFG. The relationship between MSD and the diffusion coefficients (D) is based on the related literature, as follows:

$$D = \lim_{t\to\infty}\left(\frac{MSD}{6t}\right) = \frac{1}{6}K_{MSD} \quad (2)$$

where K_{MSD} is the slope of the MSD curve.

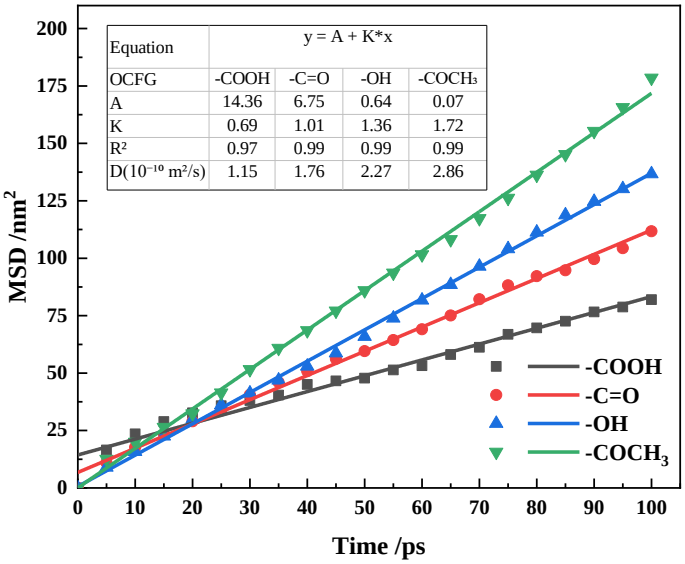

Fig. 6. MSD curves of dodecane on the DOCFG

MSD curves were used to analyze the stability of dodecane on the DOCFG. MSD curves of dodecane on the DOCFG are shown in Fig. 6. It was found that the diffusion coefficients of dodecane are 1.15×10^{-10} $m^2.s^{-1}$/ 1.76×10^{-10} $m^2.s^{-1}$/ 2.27×10^{-10} $m^2.s^{-1}$/ 2.86×10^{-10} $m^2.s^{-1}$ on the -COOH/ -C=O/ -OH / $-COCH_3$, respectively. The diffusion coefficient of dodecane on the -COOH surface is the smallest, followed by -C=O, -OH, and $-COCH_3$. However, a bigger diffusion coefficient value suggests higher dynamic properties (Wan et al., 2021). In other words, the bigger the diffusion coefficient value is, the weaker the ability to limit the diffusion of dodecane molecules is. The desorption capacities of dodecane on the surfaces of DOCFG range from strong to weak: $-COCH_3$ < -OH < -C=O < -COOH. The diffusion coefficients results agree well with the results of Interaction energy (Table 2.). Therefore, the adsorption effect of hydrocarbon oil on the OCFG surface order -COOH> -C=O >-OH >$-COCH_3$ in the absence of water.

3.3. Interactions between OCFG and dodecane molecules in the presence of water

Water is an essential medium in the flotation process (Hosseinian et al., 2020). It affects the properties of the mineral surface and the adsorption behaviors of flotation agents significantly. The water molecule cannot be ignored in the study of the interaction between dodecane and coal surface. Therefore, the adsorption behavior of dodecane at the solid-liquid interface was investigated by introducing multilayer water containing 1000 H_2O. Like the MD simulation in the absence of water, the structural, dynamic, and energetic information of the simulation systems was analyzed.

3.3.1. Adsorption configuration

The adsorption initial and equilibrium states of dodecane on the DOCFG in the presence of water were shown in Fig. 7. It can be observed from Fig. 7 that in an aqueous solution, the dodecane molecule still can adsorb on the DOCFG surfaces. But its adsorption morphology on the DOCFG surfaces is different. On the -C=O and $-COCH_3$ surfaces, dodecane appears as a monolayer with almost complete spreading. On the -OH and -COOH surfaces, dodecane appears as a multilayer and clusters together; especially on the -COOH surface, the dodecane molecules are clustered together in a spherical form. This result is significantly different from the adsorption conformation in the absence of water (Fig. 3).

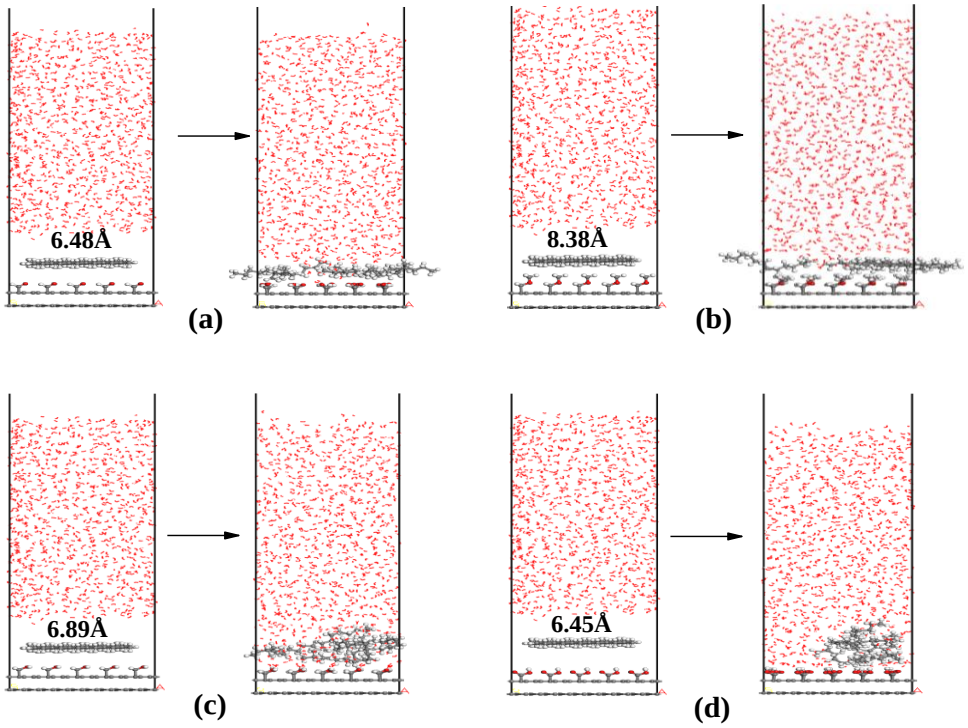

Fig. 7. The adsorption initial and equilibrium states of dodecane on the DOCFG in the presence of water (a) -C=O; (b) -$COCH_3$; (c) -OH; (d) -COOH

3.3.2. Relative concentration profiles and radial distribution function

Fig. 8 shows that the dodecane concentrations on the DOCFG surfaces differed significantly. Dodecane molecules are densely adsorbed on the -C=O and -$COCH_3$ surfaces; whereas the density on the -OH and -COOH surfaces is very low. The relative concentration of dodecane on the coal surface with DOCFG is from low to high: -COOH<-OH<-$COCH_3$<-C=O. This result is also significantly different from the result of relative concentration in the absence of water (Fig. 4).

Fig. 9 shows that there is a peak located at approximately 1.1 Å, which is the same as the peak position illustrated in Fig. 5. In addition, the peak intensities in -COOH/-OH/-$COCH_3$/-C=O are 598.83/ 578.97/ 566.56/ 548.42. The peak intensities of the -OH and -COOH surfaces are significantly

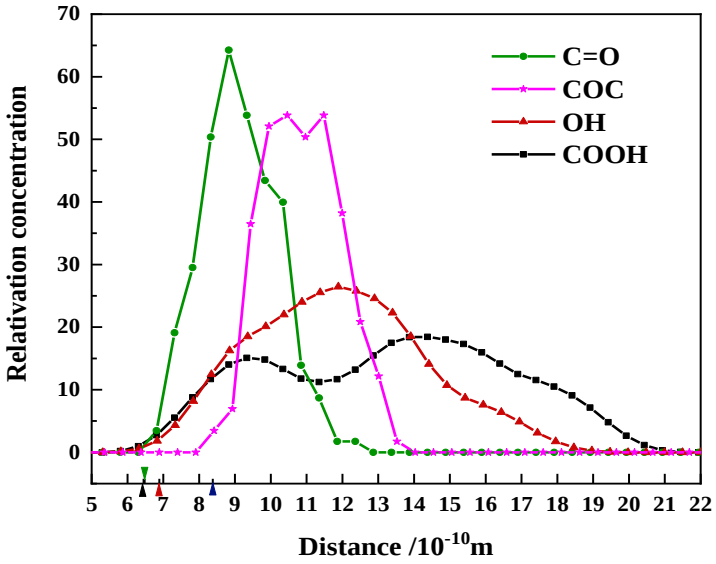

Fig. 8. The relative concentration of dodecane molecules on DOCFG

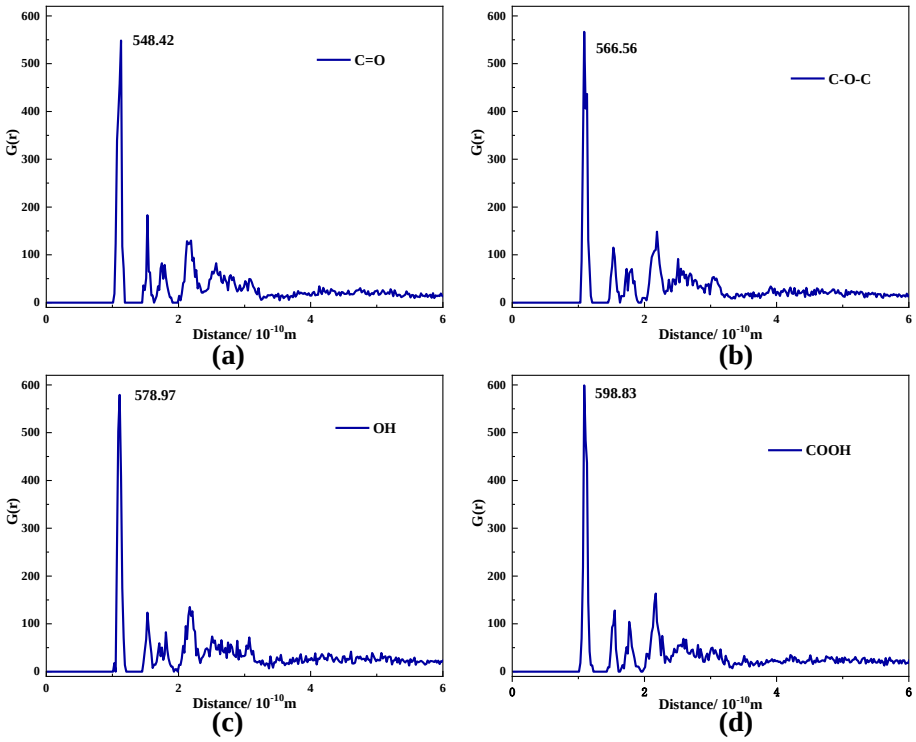

Fig. 9. Radial distribution of dodecane molecules on DOCFG

higher than those of the -C=O and -$COCH_3$ surfaces. In other words, on the -OH and -COOH surface, the probability of finding dodecane molecules around the dodecane molecule is lower at the same distance. Therefore, the strength of the interaction between the dodecane molecule and the --OH and -COOH surface is weaker. These results agree well with the results of relative concentration (Fig. 8).

3.3.3. The Diffusion Coefficients of dodecane on OCFG

MSD curves of dodecane on the DOCFG are shown in Table 3. It was found that in the presence of water, the diffusion coefficient of dodecane on the -C=O surface is the smallest, followed by -$COCH_3$, -OH, and -COOH. In other words, the desorption capacities of dodecane on the DOCFG surfaces range from strong to weak: -COOH>-OH>-$COCH_3$>-C=O. The diffusion coefficients results agree well with the results of radial distribution (Fig. 9). Therefore, the adsorption effect of hydrocarbon oil on the OCFG surface from bad to good is -COOH<-OH<-$COCH_3$<-C=O in the presence of water.

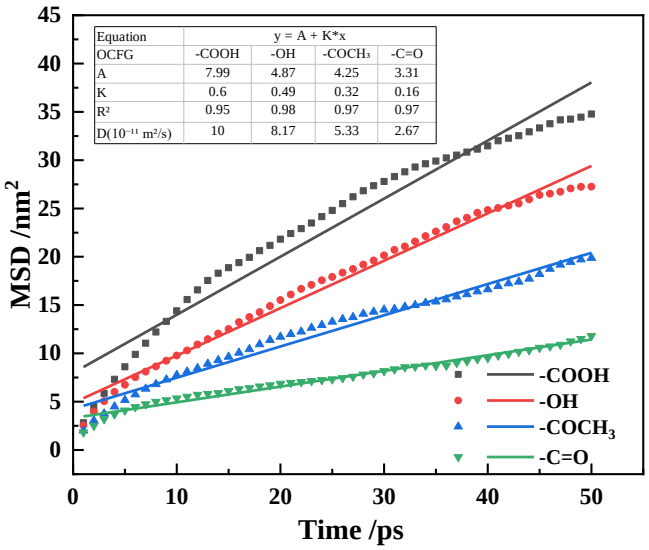

Fig. 10. Diffusion coefficients of dodecane on DOCFG

4. Discussion

Based on MDS results, it can be observed that under conditions without water, HOC has a higher affinity for -COOH, followed by the -C=O, -OH, and -$COCH_3$. In an aqueous solution, HOC has a better adsorption effect on -C=O, followed by the -$COCH_3$, -OH, and -COOH. This indicates that the water molecule has a significant effect on the interaction of the HOC with the OCFG. To further explain this phenomenon, the relative concentrations of water molecules on the DOCFG surfaces in the presence and absence of dodecane molecules were analyzed in the paper. The result is shown in Fig. 11.

It can be found from the figure that in the absence of dodecane, water molecules are capable of adsorption on the OCFG surface through hydrogen bonding (Xia et al., 2019b; Wang et al., 2017); the relative concentration of water on the OCFG surface from high to low is -COOH>-OH>-$COCH_3$>-C=O. This indicates that -COOH has a strong hydrophilic property, followed by the -OH, -$COCH_3$, and -C=O; or the OCFG hydrophobic order C=O>-$COCH_3$>-OH >-COOH. These agree with the results of previous studies (Wang et al., 2017; Wang et al., 2021). After the addition of dodecane to this system, dodecane interacts with OCFG through van der Waals forces and displaces water molecules adsorbed on the OCFG surface (Zhang et al., 2021b). This caused a decrease in the relative concentration of water on the OCFG surface; especially, on the -C=O and -$COCH_3$ surfaces, the relative concentration of water molecules decreased more significantly, followed by the -OH, -COOH. This result is consistent with the hydrophobic order of the OCFG (Wang et al., 2021).

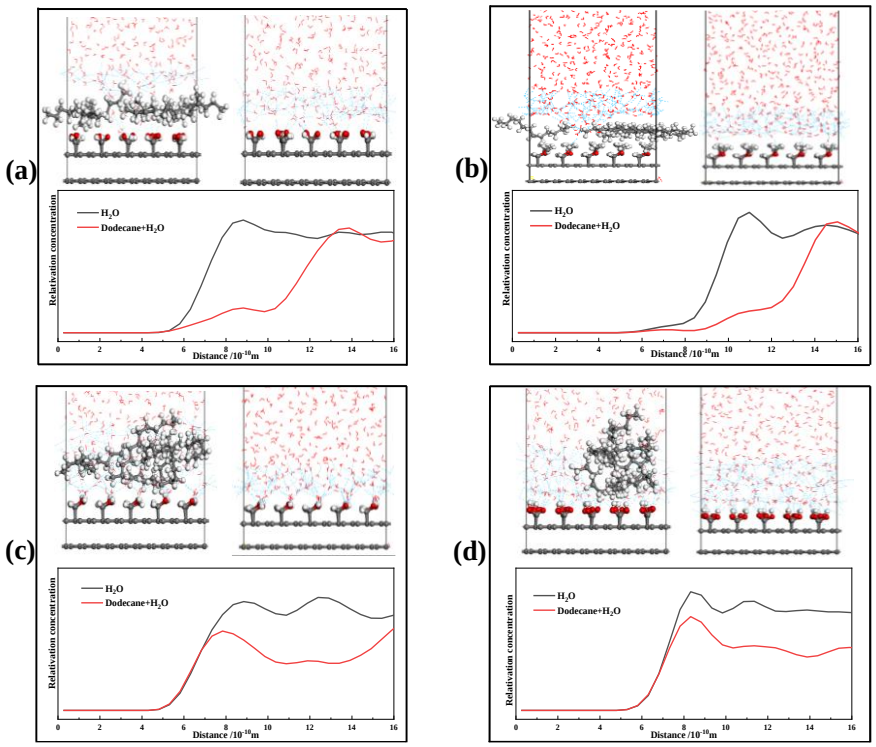

Fig. 11 The relative concentrations of water molecules on the DOCFG surfaces in the presence and absence of dodecane molecules: (a) -C=O; (b) -COCH3; (c) -OH; (d) -COOH

Moreover, MDS results of HOC on DOCFG surfaces also showed significant changes in the adsorption behavior of HOC on -COOH and -$COCH_3$ surfaces in the presence and absence of water (Fig. 6 and Fig. 10). In the absence of water, the absorption effect of HOC was best on the -COOH surface and worst on the $COCH_3$ surface. In the presence of water, the adsorption effect of HOC on the -COOH surface is the worst, the adsorption effect on the $COCH_3$ surface is substantially improving, and even the adsorption effect of HOC on the $COCH_3$ surface is better than that on the -OH surface (the adsorption of HOC on the -OH surface was better than that on the $COCH_3$ surface in the absence of water). This is because the interaction between dodecane and OCFG is dominated by the van der Waals force (Zhang et al., 2021b), and the interaction between water molecules and OCFG is dominated by hydrogen bonding (Xia et al., 2019b); the van der Waals forces are in the range of about 1 nm (Liu et al.,

2012). Hydrogen bonding makes water molecules form a hydration film at the solid-liquid interface, and the hydration layer thickness is generally within a few nanometers (Wu et al., 2016). However, in the presence of water, HOC needs to break through the hydration film to interact with the OCFG (Xia et al., 2020b). The hydration film thickness is affected by the hydrophilicity/ hydrophobicity of the solid-liquid interface (Sun et al., 2015). The stronger the hydrophilicity of the OCFG, the thicker the hydration film near the solid-liquid interface, and the more difficult it is for the HOC to break through the hydration film. If the thickness of the hydration film exceeds the distance of the van der Waals force, the HOC will not be able to break through the hydration film, not to mention the interaction with the OCFG (Zhang et al., 2021b). This indicates that the hydrophilicity of OCFG is the key factor that affects the adsorption effect of HOC on coal surfaces. In other words, the adsorption effect of HOC on the coal surface in an aqueous solution does not depend on the strength of the interaction between the OCFG and HOC in the absence of water, but on the hydrophilicity of the OCFG. Therefore, the adsorption effect order of HOC on the surface of OCFG in the presence of water is consistent with the OCFG hydrophobic order. This conclusion is beneficial to improve the coal flotation performance with hydrocarbon oil as a collector by masking the strong hydrophilic o OCFG on the coal surface. This is in good agreement with the conclusion that pre-treatment with surfactants such as dodecyl nonaethoxyl ether ($C_{12}EO_9$), carboxylic acid, and methyl acrylate improves the flotation index of low-rank coal (Zhang et al., 2021b; Zhang et al., 2021a; Guo et al., 2022).

5. Conclusions

The presence of OCFG such as -OH, -COOH, -C=O, and -$COCH_3$ on the coal surface. They affect the adsorption of HOC on coal surfaces. In conditions without water, HOC has a higher affinity for -COOH, followed by the -C=O, -OH, and -$COCH_3$. In an aqueous solution, HOC has a better adsorption effect on -C=O, followed by the -$COCH_3$, -OH, and -COOH. Moreover, the van der Waals force plays an important role in the adsorption progress of HOC on the DOCFG of coal surface. However, water molecules can be adsorbed on the OCFG surface through hydrogen bonding, further generating a hydrated film. With the increasing hydrophilicity of OCFG, the hydration film at the solid-liquid interface thickens. This causes a decrease in the chance of HOC breaking through the hydration film and interacting with OCFG. When the thickness of the hydration film exceeds the distance of the van der Waals force, the HOC will not be able to break through the hydration film, not to mention the interaction with the OCFG. These indicate that the hydrophilicity of OCFG is the key factor that affects the adsorption effect of HOC. In other words, the adsorption effect of HOC on the coal surface in an aqueous solution does not depend on the strength of the interaction between the OCFG and HOC in the absence of water, but on the hydrophilicity of the OCFG. Therefore, the -COOH and -OH on the coal surface is not conducive to the adsorption of hydrocarbon oils onto the coal surface. Masking the -COOH and -OH of the coal surface is beneficial in improving the coal flotation performance with hydrocarbon oil as a collector. This result can help to analyze the reasons for the high dosage of hydrocarbon oils when used as a collector and the poor flotation performance of coal with high OCFG. It also provides theoretical support for optimizing and designing new collectors for improved flotation performance of coal with high OCFG.

Acknowledgments

The authors are grateful for the financial support from the Shaanxi Provincial Department of Education Service Local Special Project (Grant No.21JC021), the China Scholarship Council (Grant No. 202008610058), the National Natural Science Foundation of China (Grant No. 52074206), the National Natural Science Foundation of China (Grant No. 51904222), the Natural Science Foundation of Qinghai Province, China (Grant No. 2021-ZJ-975Q), Anhui Province Key Research and Development Program Project (Grant No. 202104a07020012).

References

ABARCA, C., ALI, M. M., PELTON, R. H, 2018. *Choosing mineral flotation collectors from large nanoparticle libraries.* J. Colloid. Interf. Sci., 516, 423-430.

AKYILDIRIM, O., GÖKCE, H., BAHÇELI, S., YÜKSEK, H., 2017. *Theoretical and spectroscopic (FT-IR, NMR and UV–Vis.) characterizations of 3-p-chlorobenzyl-4-(4-carboxybenzylidenamino)-4, 5-dihydro-1H-1, 2, 4-triazol-5-one molecule.* J. Mol. Struct., 1127, 114-123.

ALISKE, M. A., ZAGONEL, G. F., COSTA, B. J., VEIGA, W., SAUL, C. K., 2007. *Measurement of biodiesel concentration in a diesel oil mixture.* Fuel, 86(10-11), 1461-1464.

ALJERF, L., NADRA, R., 2019. *Developed greener method based on MW implementation in manufacturing CNFs.* International Journal of Nanomanufacturing, 15(3), 269-289.

CAI, Y., DU, M., WANG, S., LIU, L., 2018. *Flotation characteristics of oxidized coal slimes within low-rank metamorphic.* Powder. Technol., 340, 34-38.

CHENG, G., LI, Z., MA, Z., CAO, Y., SUN, L., JIANG, Z., 2019. *Optimization of collector and its action mechanism in lignite flotation.* Powder. Technol., 345, 182-189.

DEY, S., PAUL, G. M., PANI, S. (2013). *Flotation behaviour of weathered coal in mechanical and column flotation cell.* Powder. Technol., 246, 689-694.

FAN, G., ZHANG, M., PENG, W., ZHOU, G., DENG, L., CHANG, L., LI, P., 2021. *Clean products from coal gasification waste by flotation using waste engine oil as collector: Synergetic cleaner disposal of wastes.* J. Clean. Prod., 286, 124943.

GUO, X., HE, Y., WANG, J., ZHOU, R., 2022. *Microscopic adsorption properties of methyl acrylate on lignite surface: Experiment and molecular simulation study.* Colloid. Surface. A., 641, 128468.

HARRIS, G. H., DIAO, J., FUERSTENAU, D. W., 1995. *Coal flotation with nonionic surfactants.* Coal Perparation, 16(3-4), 135-147.

HE, J., LIU, C., YAO, Y., 2018. *Flotation intensification of the coal slime using a new compound collector and the interaction mechanism between the reagent and coal surface.* Powder. Technol., 325, 333-339.

HOSEINIAN, F. S., REZAI, B., KOWSARI, E., SAFARI, M., 2020. *The effect of water recovery on the ion flotation process efficiency.* Physicochem. Probl. Miner. Process., 56, 919-927.

JIA, R., HARRIS, G. H., FUERSTENAU, D. W., 2000. *An improved class of universal collectors for the flotation of oxidized and/or low-rank coal.* Int. J. Miner. Process., 58(1-4), 99-118.

LI, B., GUO, J., LIU, S., ALBIJANIC, B., ZHANG, L., SUN, X., 2020. *Molecular insight into the mechanism of benzene ring in nonionic surfactants on low-rank coal floatability.* J. Mol. Liq., 302, 112563.

LI, P., ZONG, Z. M., WEI, X. Y., WANG, Y. G., FAN, G. X., 2019. *Structural features of liquefaction residue from Shenmu-Fugu subbituminous coal.* Fuel, 242, 819-827.

LI, Y., XIA, W., PAN, L., TIAN, F., PENG, Y., XIE, G., LI, Y., 2020a. *Flotation of low-rank coal using sodium oleate and sodium hexametaphosphate.* J. Clean. Prod., 261, 121216.

LI, Y., XIA, W., PENG, Y., LI, Y., XIE, G., 2020b. *Effect of ultrafine kaolinite particles on the flotation behavior of coking coal.* International Journal of Coal Science & Technology, 7(3), 623-632.

LI, Y., XIA, W., PENG, Y., XIE, G., 2020c. *A novel coal tar-based collector for effective flotation cleaning of low rank coal.* J. Clean. Prod., 273, 123172.

LI, H., ZHANG, K., 2019. *Dynamic behavior of water droplets impacting on the superhydrophobic surface: Both experimental study and molecular dynamics simulation study.* Applied Surface Science, 498, 143793.

LIU, Z., XIA, Y., LAI, Q., AN, M., LIAO, Y., WANG, Y, 2019. *Adsorption behavior of mixed dodecane/n-valeric acid collectors on low-rank coal surface: Experimental and molecular dynamics simulation study.* Colloid. Surface. A., 583, 123840.

LIU, Q., YUAN, S., YAN, H., ZHAO, X., 201). *Mechanism of oil detachment from a silica surface in aqueous surfactant solutions: molecular dynamics simulations.* J. Phys. Chem. B., 116(9), 2867-2875.

LYU, X., YOU, X., HE, M., ZHANG, W., WEI, H., LI, L., HE, Q., 2018. *Adsorption and molecular dynamics simulations of nonionic surfactant on the low rank coal surface.* Fuel, 211, 529-534.

QU, J., TAO, X., TANG, L., XU, N., HE, H., 2015. *Flotation characteristics and particle size distribution of micro-fine low rank coal.* Procedia Engineering, 102, 159-166.

SUN, Y., HAN, Z., LIU, H., HE, S., YANG, L., LIU, J., 2015. *Three-dimensional hotspots in evaporating nanoparticle sols for ultrahigh Raman scattering: solid–liquid interface effects.* Nanoscale, 7(15), 6619-6626.

TAN, J., CHENG, H., WEI, L., GUI, X., XING, Y., 2020. *Investigation of CTAB and DBP esters on low-rank coal flotation selectivity.* Energy. Source. Part. A., 42(10), 1225-1234.

WAN, H., YI, P., QU, J., BU, X., YANG, W., LI, H., 2021. *Adsorption Behaviors of Straight-Chain Alkanes on a Molybdenite [001]/ [100] Surface: A Molecular Dynamics Study.* Minerals, 11(5), 489.

WANG, C., XING, Y., XIA, Y., ZHANG, R., WANG g, S., SHI, K., GUI, X., 2021. *Investigation of interactions between oxygen-containing groups and water molecules on coal surfaces using density functional theory.* Fuel, 287, 119556.

WANG, J., HE, Y., PENG, Z., LING, X., WANG, S., 2017. *Estimation of hydrophilicity of coals by using the quantum chemistry calculation.* Int. J. Miner. Process., 167, 9-15.

WANG, Y., CAO, Y., LI, G., LIAO, Y., XING, Y., GUI, X., 2018. *Combined effect of chemical composition and spreading velocity of collector on flotation performance of oxidized coal.* Powder. Technol., 325, 1-10.

WU, Z., WANG, X., LIU, H., ZHANG, H., MILLER, J. D., 2016. *Some physicochemical aspects of water-soluble mineral flotation.* Adv. Colloid Interf., 235, 190-200.

XIA, W., LI, Y., NGUYEN, A. V., 2018. *Improving coal flotation using the mixture of candle soot and hydrocarbon oil as a novel flotation collector.* J. Clean. Prod., 195, 1183-1189.

XIA, W., NI, C., XIE, G., 2016. *Effective flotation of lignite using a mixture of dodecane and 4-dodecylphenol (DDP) as a collector.* Int. J. Coal. Prep. Util., 36(5), 262-271.

XIA, W., WU, F., JAISWAL, S., LI, Y., PENG, Y., XIE, G., 2021. *Chemical and physical modification of low rank coal floatability by a compound collector.* Colloid. Surface. A., 610, 125943.

XIA, W., YANG, J., LIANG, C., 2013. *Improving oxidized coal flotation using biodiesel as a collector.* International Int. J. Coal. Prep. Util., 33(4), 181-187.

XIA, Y., XING, Y., LI, M., LIU, M., TAN, J., CAO, Y., GUI, X., 2020a. *Studying interactions between undecane and graphite surfaces by chemical force microscopy and molecular dynamics simulations.* Fuel, 269, 117367.

XIA, Y., ZHANG, R., CAO, Y., XING, Y., GUI, X., 2020b. *Role of molecular simulation in understanding the mechanism of low-rank coal flotation: A review.* Fuel, 262, 116535.

XIA, Y., ZHANG, R., XING, Y., GUI, X., 2019. *Improving the adsorption of oily collector on the surface of low-rank coal during flotation using a cationic surfactant: An experimental and molecular dynamics simulation study.* Fuel, 235, 687-695.

XIA, Y., YANG, Z., XING, Y., GUI, X., 2019. *Molecular simulation study on hydration of low-rank coal particles and formation of hydration film.* Physicochem. Probl. Miner. Process., 55, 586-596.

XIE, W., HAN, Y., TAI, S., 2017. *Biodiesel production using biguanide-functionalized hydroxyapatite-encapsulated-γ-Fe2O3 nanoparticles.* Fuel, 210, 83-90.

XU, M., XING, Y., CAO, Y., GUI, X., 2019. *Waste colza oil used as renewable collector for low rank coal flotation.* Powder. Technol., 344, 611-616.

YANG, Z., LIAO, Y., REN, H., HAO, X., SONG, X., LIU, Z., 2021. *A novel co-treatment scheme for waste motor oil and low rank coal slime: Waste dispose waste.* Fuel, 292, 120275.

ZHANG, L., GUO, J., XIE, Z., LI, B., LIU, S., 2021a. *Micro-mechanism of improving low-rank coal flotation by using carboxylic acid collector: A DFT calculation and MD simulation study.* Colloid. Surface. A., 622, 126696.

ZHANG, L., GUO, J., HAO, M., LI, B., LIU, S. 2021b. *Microscopic spreading characteristics of non-polar oil droplet on low rank coal surface: Effects of surfactant pretreatment and oxygen-containing groups.* J. Mol. Liq., 325, 115232.

ZHANG, L., LI, B., XIA, Y., LIU, S., 2017. *Wettability modification of Wender lignite by adsorption of dodecyl poly ethoxylated surfactants with different degree of ethoxylation: A molecular dynamics simulation study.* J. Mol. Graph. Model., 76, 106-117.

ZHANG, L., SUN, X., LI, B., XIE, Z., GUO, J., LIU, S., 2020a. *Experimental and molecular dynamics simulation study on the enhancement of low rank coal flotation by mixed collector.* Fuel, 266, 117046.

ZHANG, R., XING, Y., XIA, Y., GUO, F., DING, S., TAN, J., GUI, X., 2020b. *Synergistic adsorption mechanism of anionic and cationic surfactant mixtures on low-rank coal flotation.* ACS omega, 5(32), 20630-20637.

ZHANG, R., XING, Y., XIA, Y., LUO, J., TAN, J., RONG, G., GUI, X., 2020c. *New insight into surface wetting of coal with varying coalification degree: An experimental and molecular dynamics simulation study.* Appl. Surf. Sci., 511, 145610.

ZHANG, W., XIA, W., 2015. *The deashing of high-ash coking coal fines by flotation.* Energy. Source. Part. A., 37(7), 714-720.

ZHOU, Y., ALBIJANIC, B., WANG, Y., YANG, J., 2018. *Characterizing surface properties of oxidized coal using FTIR and contact angle measurements.* Energy. Source. Part. A., 40(12), 1559-1564.

ZHU, D., MIAO, S., XUE, B., JIANG, Y., WEI, C., 2019. *Effect of coal gasification fine slag on the physicochemical properties of soil.* Water, Air, & Soil Pollution, 230(7), 1-11.

ZHU, X. N., WANG, D. Z., NI, Y., WANG, J. X., NIE, C. C., YANG, C., LI, L., 2020. *Cleaner approach to fine coal flotation by renewable collectors prepared by waste oil transesterification.* J. Clean. Prod., 252, 119822.